

See discussions, stats, and author profiles for this publication at: <https://www.researchgate.net/publication/41026946>

Cross-Talk-Free Dual-Color Fluorescence Cross-Correlation Spectroscopy for the Study of Enzyme Activity

ARTICLE *in* ANALYTICAL CHEMISTRY · FEBRUARY 2010

Impact Factor: 5.64 · DOI: 10.1021/ac9024768 · Source: PubMed

CITATIONS

7

READS

15

6 AUTHORS, INCLUDING:



Yong-Il Lee

Taipei Veterans General Hospital

233 PUBLICATIONS 3,405 CITATIONS

SEE PROFILE



Prescott Deininger

Tulane University

218 PUBLICATIONS 15,490 CITATIONS

SEE PROFILE



Steven Soper

Louisiana State University

201 PUBLICATIONS 5,507 CITATIONS

SEE PROFILE

Published in final edited form as:

Anal Chem. 2010 February 15; 82(4): 1401–1410. doi:10.1021/ac9024768.

Cross-Talk Free Dual-Color Fluorescence Cross-Correlation Spectroscopy (FCCS) for the Study of Enzyme Activity

Wonbae Lee¹, Yong-Ill Lee², Jeonghoon Lee¹, Lloyd M. Davis³, Prescott Deininger⁴, and Steven A. Soper^{*,1}

¹ Department of Chemistry, Louisiana State University, Baton Rouge, Louisiana 70803-1804, USA

² Department of Chemistry, Changwon National University, Changwon, 641-773, South Korea

³ Center for Laser Applications, University of Tennessee Space Institute, Tullahoma, TN 37388, USA

⁴ Tulane University, Department of Epidemiology and Tulane Cancer Center, New Orleans, LA 70112, USA

Abstract

We have developed an instrument for spectral cross-talk free dual-color fluorescence cross-correlation spectroscopy (FCCS), which provides a readout modality for the study of enzyme activity in application areas such as high throughput screening. Two spectrally distinct (~250 nm) fluorophores, Cy3 and IRD800, were excited simultaneously using two different excitation sources; one poised at 532 nm and the other at 780 nm. The fluorescence information was processed on two different color channels monitored with single photon avalanche diodes (SPADs) that could transduce events at the single-molecule level. The system provided no color cross-talk (cross-excitation and/or cross-emission) and/or fluorescence resonance energy transfer (FRET), significantly improving data quality. To provide evidence of cross-talk free operation, the system was evaluated using bright microspheres ($\lambda_{\text{abs}} = 532$ nm, $\lambda_{\text{em}} = 560$ nm) and quantum dots ($\lambda_{\text{abs}} = 532$ nm, $\lambda_{\text{em}} = 810$ nm). Experimental results indicated that no color leakage from the microspheres or quantum dots into inappropriate color channels was observed. To demonstrate the utility of the system, the enzymatic activity of APE1, which is responsible for nicking the phosphodiester backbone in DNA on the 5' side of an apurinic/apyrimidinic site, was monitored by FCCS using a double-stranded DNA substrate dual labeled with Cy3 and IRD800. Activity of APE1 was also monitored in the presence of an inhibitor (7-nitroindole-2-carboxylic acid) of the enzyme using this cross-talk free FCCS platform. In all cases, no spectral leakage from single molecule events into inappropriate color channels was observed.

Introduction

Fluorescence correlation spectroscopy (FCS) or fluorescence fluctuation spectroscopy (FFS) have emerged as sensitive techniques to monitor a variety of biochemical reactions, such as protein-protein interactions,¹⁻² reaction kinetics,³⁻⁴ and equilibrium concentrations.⁵⁻⁶ FCS was introduced more than 35 years ago to measure diffusion and chemical dynamics of DNA-drug interactions through the analysis of concentration fluctuations about the equilibrium of a

* To whom correspondence should be addressed. chsoper@lsu.edu.

Supporting Information **Available:** (1) Raw data streams for concentration changes; (2) detailed results of the characterization experiments for different flow rates; (3) data streams of blank buffer to select a threshold for minimizing counting errors; (4) Raw data streams when the concentration of two nanoparticles was increased so that they are often present in the same excitation volume; and (5) MALDI spectrum of Cy3-labeled oligonucleotides, IRD800-labeled oligonucleotides, and APE1.

small ensemble ($\sim 10^3$) of molecules.⁷ Recently, FCS has been applied as a tool to screen for protein interactions for both fundamental research and drug development/discovery applications due to its noninvasiveness, single-molecule limits-of-detection, rapid readout, high analytical sensitivity and accessibility to physical and chemical information at the single-molecule level free from ensemble averaging.⁸⁻¹⁰

The common instrumental setup for a FCS experiment consists of a laser beam with a Gaussian profile, which is directed into a microscope objective possessing a high numerical aperture and focused into an aqueous solution containing molecules under study that are labeled with a fluorescent dye. The focused laser beam creates a small open volume element called the probe volume. The temporal average of the particle number inside the probe volume is typically between 0.1 and 1,000 for FCS or FFS.¹¹ The occupancy number fluctuates about its equilibrium value as molecules diffuse in and out of the probe volume or as fluorescent molecules are chemically transformed to and from non-fluorescent species undergoing enzymatic processing. The temporal autocorrelation of the fluorescence signal fluctuation yields the time scale of such dynamics and its variance provides the average number of independent fluorophores ($\langle N \rangle$) in the probe volume.¹²

Most applications of FCS are based on the analysis of the molecular dynamics and the reaction kinetics of fluorescently-labeled biomolecules that undergo temporal changes in their diffusion properties. However, when analyzing an enzymatic reaction, the change in mass between enzyme and enzyme-substrate complex are usually small and thus, not recognizable due to the logarithmic time-scale of the diffusion calculated by the Stokes-Einstein equation.¹¹

To overcome this, a substrate molecule can be labeled with two spectrally distinguishable fluorophores and the molecular changes invoked on this substrate, for example by an enzyme, monitored using Fluorescence Cross Correlation Spectroscopy (FCCS). For example, a double-stranded DNA substrate was labeled with a red (Cy5) and green (Rhodamine green) dye at opposite ends and the restriction endonuclease, *Eco* RI, was added to clip the DNA at an internal sequence recognition site. Due to the site specific breaks induced by *Eco* RI, the number of doubly-labeled DNA substrate molecules decreased successively with the enzyme reaction progress.¹³ This process is called dual-color FCS (dcFCS) or simply FCCS.¹²⁻¹⁴ The normalized cross-correlation function, $G_c(\tau)$, is calculated as the time average of the product of the fluorescence fluctuations of two species, i at times t and j at $t + \tau$, normalized by the product of the time-averaged fluorescence signals of the two species i and j (see equation 1).^{12, 15}

$$G_c(\tau) = \frac{\langle \Delta I_i(t) \Delta I_j(t+\tau) \rangle}{\langle I_i(t) \rangle \langle I_j(t) \rangle} = \frac{\langle \Delta I_1(0) \Delta I_2(\tau) \rangle}{\langle I_1(t) \rangle \langle I_2(t) \rangle} + 1 \quad (1)$$

The angular brackets ($\langle \rangle$) indicate averaged values, I is the fluorescence signal as a function of time, and τ is the delay time. Compared to FCS in which a single autocorrelation function where $i = j$, cross-correlation functions use $i \neq j$ as shown in equation (1). Other detailed mathematical relationships for FCCS can be found in the literature.^{4, 12, 16-17}

When performing FCCS measurements, special considerations to cross-excitation, cross-emission, and fluorescence resonance energy transfer (FRET) must be provided, which in many cases requires additional mathematical processing to prevent false positive signals arising from spectral leakage and to improve data quality.¹⁸ These issues are typically a result of the broad

excitation/emission envelopes associated with most molecular dyes. For example, if cross-emission occurs in a FCCS measurement, a series of negative control experiments with the same sample concentrations are required to determine cross-talk parameters, such as the bleed-through ratio used to correct the impaired data.¹⁹⁻²⁰ If there are only cross-excitation and/or FRET, coincidence events can be considered as truly double-labeled molecules whatever the excitation rate or FRET efficiency. However, cross-excitation and/or FRET may cause other problems in FCCS, such as photobleaching.²⁰⁻²¹

To solve issues associated with cross-talk in FCCS, new methodologies have been suggested, such as single laser wavelength FCCS (SW-FCCS),²² two-photon excitation,²³⁻²⁵ two alternating pulsed excitation,²⁶ and switching FCCS.²¹ For example, Hwang *et al.* proposed SW-FCCS using a single laser excitation beam at 488 nm to excite a combination of labels emitting at 510 nm and 695 nm.²² Unfortunately, cross-talk was not completely suppressed. While the aforementioned methods were fairly successful at minimizing spectral cross-talk, additional mathematical compensation steps were still required.²⁷ Although cross-talk can be corrected quantitatively,¹⁹⁻²⁰ the corrections are rather provisional, complex, and time-consuming.

Recently, Thews *et al.* successfully eliminated cross-talk signals in their FCCS measurements by adopting an acousto-optic modulator (AOM)-based pulse picker system to generate alternating pulsed excitation laser beams of different colors interleaved with a 50 ns spacing.²⁶ The elimination of cross-talk was accomplished through differences in the dye's finite upper state lifetimes. More recently, Takahashi *et al.* demonstrated the feasibility of cross-talk-free, switching FCCS system using acousto-optic tunable filters (AOTFs) in the excitation laser to produce precise alternating laser beams for the study of the activity of caspase-3.²¹ Both of these techniques required modulators and in some cases pulsed lasers, which increased the complexity of the optical system and required post-processing of the data to synchronize the time course of the alternating detected signals.

We present in this work a simple dual-color FCCS system capable of studying bioreactions to provide near real-time results using continuous wave dual excitation that negated the need for mathematical compensations/post-processing steps through the use of a chromophore set with widely divergent excitation/emission maxima (Cy3 and IRD800) to provide cross-talk free dual-color FCCS. Due to the large spectral separation (~250 nm), cross-talk and FRET between the two dyes and color channels was completely suppressed. The system was evaluated using a model system, in this case monitoring the activity of the enzyme, APE1 (also known as Hap1, Apex, and Ref-1), which is responsible for >95% of the nicking activity of the phosphodiester backbone in DNA on the 5' side of an apurinic/apyrimidinic site.²⁸⁻²⁹

Experimental Details

Materials

The 5'-Cy3-labeled oligonucleotide containing an abasic site (5'-Cy3-GCCCCXGGGGACGTACGATATCCCGCTCC-3', X is Tetrahydrofuran, an abasic site analog, MW = 9485.9 Da) was custom-synthesized by Midland Certified Reagent Company (Midland, TX) and used as received. Its complementary oligonucleotide was labeled with IRD800 on its 5' end (5'-IRD800-GGAGCGGGATATCGTACGTCCCCCGGGGC-3', MW = 10152.1 Da) and was synthesized by Integrated DNA Technology (Coralville, IA). AP endonuclease APE1, (MW = 35,555 Da³⁰) was kindly donated by Dr. P. L. Deininger (Tulane Cancer Center, LA). The APE1 inhibitor, CRT0044876 (7-nitroindole-2-carboxylic acid), was purchased from Cole-Parmer (Vernon Hills, IL) and used after dissolving in DMSO.

Carboxylate-modified fluorescent microspheres (0.2 μm in diameter, F8809, Molecular Probes, Eugene, OR) were used to initially evaluate the 560 nm color channel and aid in the evaluation of system performance due to their superior photostability and brightness. Commercially available PbS Quantum Dots (ED-P20-TOL-0850, PbS Core EviDots, Evident Technologies, Troy, NY) were chosen for the optimization of the 810 nm color channel. These quantum dots have a nominal diameter of 2.2 nm ($\lambda_{\text{abs}} < 700$ nm, $\lambda_{\text{em}} = 850$ nm, $\epsilon_{\text{ext}} = 2.00 \times 10^4/\text{mol}$) and were shipped in toluene at concentrations of 2.5 mg/ml. The fluorescent samples were diluted with HPLC grade water to avoid high background from contaminated buffer solutions and vortexed for ~ 3 min to minimize aggregation prior to use. Unless otherwise specified, the study of APE1 enzyme activity was performed at 37°C in BER buffer containing 50 mM Tris (pH 8.0), 1 mM MgCl_2 , 50 mM NaCl and 2 mM dithiothreitol (DTT).

Instrumentation

Both the 532 nm green solid-state laser (GTEC-500-532-10, Lasiris, Inc., Quebec, Canada) and the 780 nm diode laser (GH0781JA2C, Thorlabs, Newton, NJ) were filtered spectrally with laser line filters (FL532-10 for 532 nm, and FL780-10 for 780 nm, FWHM = 10 ± 2 nm, Thorlabs, Newton, NJ) and combined by reflecting the 532 nm laser using a dichroic mirror (Z532RDC, Chroma Technologies, Rockingham, VT) as shown in Figure 1a. The collimated excitation beams were focused through a 40 \times , 0.75 NA objective (MRH00400, Plan fluor, Nikon) into the sample container, which consisted of a 50 μm internal diameter fused silica capillary (TSP050192, Polymicro Technologies, Phoenix, AZ) that was mounted on an XYZ micro-translational stage for positioning the capillary with respect to the laser beam and collection optics. The length of the detection window, formed by removing the polyimide coating of the capillary, was ~ 1 cm. Sample solutions were delivered through the capillary using a Harvard apparatus model 22 syringe pump (South Natick, MA). Both lasers were operated with an average power of 50 μW as measured at the flow cell. A custom-designed dichroic mirror (Z532/780RPC, Chroma Technologies, Rockingham, VT) was used to reflect the collimated excitation beams through the objective and focused into the detection window of the capillary by positioning the dichroic mirror at a 45° angle of incidence. The dual-color fluorescence emission resulting from Cy3 ($\lambda_{\text{abs}} = 532$ nm, $\lambda_{\text{em}} = 560$ nm) and IRD800 ($\lambda_{\text{abs}} = 780$ nm, $\lambda_{\text{em}} = 810$ nm) were collected by the same objective, transmitted through the dichroic mirror and sorted by a second dichroic mirror (640DCSPXR, Chroma Technologies, Rockingham, VT) into one of two detection channels with observation wavelengths centered at 560 nm and 810 nm. For the 560 nm detection channel, a short-pass filter (720SP-2P, Chroma Technologies, Rockingham, VT) and a band-pass filter (XB97, 560BP10, Omega Optical, Brattleboro, VT) centered at 560 nm with a 10 nm bandwidth (FWHM) were used to isolate the green fluorescence as shown in Figure 1b. Similarly, the 810 nm detection channel had an 800 nm long-pass filter (HQ800LP, Chroma Technologies, Rockingham, VT) and a band-pass filter (810DF10, Omega Optical, Brattleboro, VT) centered at 810 nm with a 10 nm bandwidth (FWHM).

The filtered fluorescence was then focused onto the active area (175 μm) of two separate single photon avalanche diodes (SPCM-AQR-14, EG&G, Vandreuil, Canada) using a 20 \times objective (MRH00200, Plan fluor, Nikon). Dark count rates for the SPCMs were < 100 cps according to the manufacturer. The avalanche pulses from the SPCMs were fed into a counter/timer computer board (PCI-6602, National Instruments, Austin, TX) having a temporal resolution of 12.5 ns and subsequently analyzed with custom-built software written using LabVIEW 7.0 (National Instruments, Austin, TX) by measuring the green and red color signals simultaneously and cross-correlating them. FCCS experiments were performed for 20 s for each sample, and the auto- and cross-correlation functions on the data streams calculated. Details on the data acquisition software and algorithm for the calculation of the auto-correlation

and cross-correlation functions from single molecule photon burst events has been described previously.³¹

MALDI analysis of the enzymatic products of the APE1 nicking reaction

A 75 mg/ml solution of 3-hydroxy-picolinic acid (3-HPA) was prepared in 50% acetonitrile to serve as a MALDI matrix. Sample spots on a MALDI target plate were made by combining 1 μ l of a sample solution at 10 μ M with 2 μ l of the matrix. Mass spectra of the enzyme reactions were recorded on a Bruker ProFLEX MALDI-TOF mass spectrometer (Bruker Daltonik, Bremen, Germany) operated in a linear mode with a pulsed nitrogen laser (337 nm, pulse frequency, 2 Hz). The total acceleration voltage was 20 kV. Negative ions were detected and approximately 100 single-shot spectra were acquired for each sample spot. Data processing was performed with XMASS 5.0 provided by the mass spectrometer manufacturer.

Results and Discussion

Evaluation of system performance

We first used fluorescent nanoparticles to aid in the initial evaluation of system performance in terms of color cross-talk due to their high brightness and favorable photostabilities. The dual-color optical system parameters were investigated using 200 nm fluorescent spheres for the green channel and quantum dots for the near-IR channel.

The FCCS dual-color system was first characterized in terms of the single molecule delivery rate and its effects on detection limit and processing throughput. If the occupancy probability of particles is low (<1), which is adjusted using the proper concentration range, the number of fluorescence events observed should increase linearly with solution velocity ($N_{ev} = (2P_v vT)/(\pi\omega_0)$).³² Conversely, the average transit time decreases with increasing flow rate due to the reciprocal relationship between the velocity and the transit time ($\tau_t = (\pi\omega_0)/(2v)$), which results in a decrease in the signal-to-noise ratio.³² A microsphere sample of 4.5×10^5 particles/ml was injected into the sampling capillary at different flow rates ranging from 1.0 μ l/min ($v = 0.84$ cm/s) to 4 μ l/min ($v = 3.39$ cm/s). As can be seen from Figures 2a-2d, the width of the fluorescence burst response was highly dependent upon the linear velocity. In addition, the linear dependence of transit time on flow rate was observed (data not shown) as determined from the autocorrelation function (see Figure 2e) and also, the number of photon burst events as a function of particle concentration and particle velocity (see Figures S1 and S2 in the Supporting Information).³³

The number of detected fluorescence burst events increased linearly ($R^2 = 0.994$, $n = 5$) with flow rate at a fixed particle concentration (see Figure S2). For the data shown in Figure 2, each event was determined to arise from a single particle due to statistical considerations. To perform these measurements, a preset threshold value was selected, which was determined by evaluating data from buffer solutions only (see Figure S3 in the Supporting Information) and selected to produce a false positive rate of 0 per data stream. An event was scored as a positive event only when its intensity exceeded this selected threshold level (20,000 cps).

Cross-talk evaluation using single particle detection

One of the most common challenges associated with FCCS is cross-talk between detection channels, which results from overlap in the broad absorption and/or emission spectra of the fluorescent dyes used to report on enzyme activity and the inefficiency in spectral sorting by the optical filters.^{19-21, 26, 34} Here, we utilized Cy3 emitting fluorescence at 560 nm with IRD800 emitting fluorescence at 810 nm as the dye pair, which could potentially provide cross-talk free dual-color FCCS due to their large spectral separation (~ 250 nm) of this dye set.

To initially demonstrate the extent of cross-talk and/or spectral leakage between the two color channels, fluorescent spheres and quantum dots were employed. A mixture of microspheres ($\lambda_{\text{abs}} = 532 \text{ nm}$, $\lambda_{\text{em}} = 560 \text{ nm}$) and quantum dots ($\lambda_{\text{abs}} < 700 \text{ nm}$, $\lambda_{\text{em}} = 850 \text{ nm}$) were excited by a single laser source (532 nm). Two spectrally different emissions were monitored; one at 560 nm resulting from the fluorescent spheres and another at 810 nm associated with the quantum dots. Because these nanoparticles are brighter than organic fluorophores, any cross-talk or signal leakage, if present, could be monitored with high sensitivity.

In order to check for spectral leakage into the 810 nm channel, a microsphere sample of 4.5×10^5 particles/ml was injected into the capillary while simultaneously collecting burst signals in both color-channels. Figure 3a shows fluorescence bursts generated for single microspheres entering the probe volume obtained on the 560 nm detection channel (top). Even though strong burst signals were observed in the 560 nm channel, no cross-talk signals were observed in the 810 nm detection channel (bottom, with negative counts used for easy visualization). To check the other channel for spectral leakage, the quantum dot sample was next introduced into the capillary and signals on both color channels were again monitored. As can be seen in Figure 3b, the quantum dots produced distinct burst signals only in the 810 nm detection channel with no observable signals observed in the 560 nm detection channel. Based on these experimental results, we concluded that the two different emissions at 560 nm and 810 nm were completely sorted and monitored on each assigned channel without any observable signal leakage/crosstalk.

Analysis of cross-correlation functions

For initial testing of two-color FCCS operation, the fluorescent spheres and quantum dots were mixed and injected into the sampling capillary. Figure 3c shows burst data for this mixture at the two monitored wavelengths (top for 560 nm detection channel and bottom for the 810 nm detection channel). As can be seen in the trace data, the bursts appeared to be non-correlated in time, indicating that they did not associate and were independent (number of coincident events exceeding a threshold level of 20,000 cps = 0). The independent transport of these two particles was also verified by calculating the cross-correlation function (see Figure 3d) using equation 1, which averages the arrival times over all events occurring within the data stream for 20 s and is a sensitive indicator of correlated signals. In the analysis of the cross-correlation function, I_1 and I_2 represent fluorescence intensities of the spheres (560 nm) and quantum dot (810 nm). Inspection of Figure 3d indicated the absence of any meaningful cross-correlation for these extremely bright particles, which would result from spectral leakage into inappropriate color channels or random coexistence of two independent nanoparticles in the probe volume. Based on Poisson probability statistics,³⁵ the probability of spheres using a particle concentration of 8.6×10^4 particles/ml in the probe volume ($\sim 0.6 \text{ pL}$) was $\sim 0.005\%$ and the probability (concentration = $1.0 \times 10^{-9} \text{ mg/mL}$) of quantum dots was $\sim 0.89\%$. The coincidence probability of the two nanoparticles was therefore $4.5 \times 10^{-5}\%$ indicating low probability of both particles simultaneously residing within the probe volume (see Figure 3c). However, when the coincidence probability (0.0825%) of the two nanoparticles was increased simply by increasing the concentration of these particles, an observable cross-correlation function was found between the two color channels as shown in Figure 3e (see also Figure S4 in the Supporting Information).

Investigating Cross-talk/FRET using Cy3 and IRD800 labeled dsDNA

Although no cross-talk between the two color channels was observed from the nanoparticle experiments, most organic dyes have broad excitation/emission envelopes that can create a situation where cross-talk (cross-excitation or cross-emission) and/or FRET are present, which is a typical problem in most FCCS studies requiring additional control measurements and post-mathematical processing of the data to minimize “false positive” results.^{18-19, 36-37} In the next

set of experiments, we sought to verify the extent of cross-talk and/or FRET for two fluorescent organic dyes as opposed to fluorescent spheres or quantum dots. Two different fluorophores (Cy3 and IRD800) were identified as possible candidates due to their characteristic fluorescence wavelengths matching the selected observation wavelengths (560 nm and 810 nm) of our system. Both excitation wavelengths (532 nm and 780 nm) were made colinear and directed into the sampling capillary that was filled with a dsDNA oligonucleotide labeled with Cy3 and IRD800 on their respective 5' ends with the emission monitored simultaneously in both color channels. Figure 4a shows the resulting response monitored by the two color channels. The presence of the double-labeled dsDNA could be confirmed through coincident events on both color channels. However, the data integrity of these coincident events could be impaired by cross-emission of an independent dye (normally excited by a shorter wavelength) requiring a series of negative control experiments with the same sample concentrations as used in Figure 4a to determine the cross-talk parameters, such as the bleed-through ratio, in order to correct for the impaired data.¹⁹⁻²⁰

To demonstrate the elimination of cross-talk and FRET in this FCCS scheme, one of the excitation lasers was simply switched off at ~10 s while detecting emission signals on both detection channels from the dsDNA sample (see Figures 4b and 4c). Figure 4b shows the resulting response produced by switching off the 780 nm excitation laser ~10 s into the measurement. As can be seen from Figure 4b, only the Cy3 fluorescence was observed in the 560 nm detection channel (top) with no apparent signal seen in the 810 nm detection channel (bottom), indicative of no cross-excitation of IRD800 by the 532 nm laser nor cross-emission of the Cy3 fluorescence into the 810 nm channel. Furthermore, due to large differences (~250 nm) between potential donor emission and acceptor excitation, photon events in the 810 nm detection channel, which would result from FRET, were also not observed at least up to the concentration range tested. As it is not allowed due to energetic reasons,²⁰ inspection of the 560 nm detection channel response when the 532 nm beam was switched off at ~10 s into the run indicated no cross-emission of signal from IRD800 into the 560 nm detection channel and also, no cross-excitation of Cy3 by the 780 nm excitation source (see Figure 4c).

Figure 4d shows the auto-correlation and cross-correlation functions when a Cy3-labeled ssDNA sample was injected into the system showing that no auto-correlation could be seen in the 810 nm detection channel. When an IRD800-labeled ssDNA sample was analyzed, no correlation in the autocorrelation function for the 560 nm detection channel was observed as can be seen in Figure 4e.

Measurement of APE1 activity using dual-color FCCS

As a model for the utility of this dual-color FCCS instrument for monitoring enzyme activity, an endonuclease nicking reaction of a dsDNA substrate having an abasic site was employed as a substrate for APE1, which recognizes an apurinic/apuridinic (AP) site in the mammalian base excision repair (BER) pathway and cleaves the phosphodiester backbone in DNA on the 5' side of the apurinic/apyrimidinic site. The activity of APE1 against AP sites, which are a major form of DNA damage resulting from hydrolysis of the *N*-glycosylic bond on dsDNA, has been studied.²⁸⁻²⁹ dsDNA substrates were formed by hybridizing two synthetic 30 nt complementary oligonucleotides, which were labeled with Cy3 and IRD800 on their respective 5' ends. The 30 bp duplex oligonucleotide containing the abasic site at position 7 in the upper strand was selected so that the intact 30 bp duplex did not denature at room temperature, but following nicking by APE1 to generate a 6-mer, could denature at room temperature to generate two fragments with each containing the Cy3 or IRD800 fluorophore (see Figure 5a). The intact dsDNA substrate will generate coincident events in the two-color channels. APE1 will nick dsDNA at the AP site into a smaller fragment that will melt at room temperature due to the decreased thermodynamic stability in the presence of APE1 compared to the case when no

APE1 was present due to differences in their respective T_m 's (T_m , nicked 6-mer $\sim -2.6^\circ\text{C}$, T_m , nicked 24-mer $\sim 71.6^\circ\text{C}$, and T_m , intact 30-mer $\sim 78.7^\circ\text{C}$, as calculated by the DINAMelt Software³⁸) into a single-stranded DNA fragment that carries one of the fluorescent labels resulting in an increase in the number of non-coincident events.

The oligonucleotides were hybridized at 0.3 pM in a BER reaction buffer. A series of solutions containing the hybridized duplexes were prepared by adding APE1 enzyme and in some cases, an inhibitor as well. The reaction mixtures were incubated at 37°C for 30 min and a FCCS analysis was initiated by pumping the reaction mixtures through the sampling capillary. As shown in Figure 5b, the amplitude of the cross-correlation function in the absence of APE1 was reduced when APE1 was added to the reaction mixture indicating nicking of the dsDNA substrate by APE1 (see the raw data traces in Figure 5c). However when the inhibitor, CRT0044876, was added to APE1 enzyme, the amplitude of the cross-correlation function was partially recovered representing decreased activity of the APE1 enzyme. The intact and nicked dsDNA substrates by APE1 were also distinguished by differences in the number of coincident events as monitored by the Cy3 and IRD800 color channels (see Figure 5d). As expected, no coincident events resulting from spectral cross-talk were found when only a Cy3 ssDNA or IRD800 ssDNA sample were analyzed (see Figure 5d). If coincident events were observed for the ssDNA fluorescently-labeled substrates, a series of negative control experiments and mathematical corrections would be necessary to minimize false positive signals.¹⁹⁻²⁰ As noted by Bacia *et al.*,¹⁹ a sample containing a green wavelength dye excited by a shorter excitation wavelength should be measured to determine the bleed-through ratio ($k_{\text{Gr}} = \text{count rate in the green channel}/\text{count rate in the red channel}$) at the same sample concentration, but only in the case of unidirectional cross-talk from the green dye. However, these correctional procedures were not necessary in this FCCS scheme because there was no cross-talk and/or FRET (see Figures 4b-4e and 5c).

MALDI analysis of the enzymatic products by APE1

To confirm that APE1 nicked the appropriate AP site, 6-mer (2219.7 Da) and 24-mer (7266.2 Da) APE1 products were analyzed by matrix-assisted laser desorption ionization time-of-flight mass spectroscopy (MALDI-TOF MS) in the negative-ion mode. A matrix was required to yield high quality DNA MALDI results; 3-hydroxypicolinic acid (3-HPA) was chosen due to its demonstrated utility for DNA analysis using MALDI.³⁹ The 6-mer and 24-mer APE1 products were successfully confirmed by comparing the MALDI mass spectrum of the intact Cy3-labeled oligonucleotide sample as shown in Figure 5e (see also Figure S5 in the Supporting Information for the MALDI spectrum of Cy3-labeled oligonucleotides, IRD800-labeled oligonucleotides, and APE1). The three major signals observed in the spectrum corresponded to singly and doubly charged ions of the 24-mer (7.3 kDa and 3.6 kDa) and a singly charged ion for the 6-mer (2.2 kDa) that arise from the precise nicking of APE1 at the abasic site, which occurred at position 7 in the upper strand. The mass spectrum of a pristine Cy3-labeled or IRD800-labeled 30-mer oligonucleotide sample without APE1 is shown in Figure S5 (see Supporting Information). Although poorly resolved, weak high-mass shoulders associated with each of the major peaks were observed, which are common in DNA MALDI analysis due to the formation of analyte-matrix adducts.⁴⁰ These results confirmed that AP endonuclease nicked the AP site without breaking other phosphodiester bonds in the substrate.

Conclusions

A cross-talk free dual color FCCS instrument using simultaneous excitation of two fluorophores (Cy3/IRD800) spectrally separated by ~ 250 nm was designed and demonstrated by monitoring the enzyme activity of APE1 using a dsDNA substrate that was labeled with Cy3 and IRD800 that possessed an abasic site. Characterization experiments using bright

fluorescent spheres and quantum dots indicated no cross-talk or FRET between the two color channels due to the large spectral differences in their absorption/emission maxima. In addition, signal leakage of fluorescence from organic dye molecules into inappropriate color channels resulting from crosstalk or FRET was not observed as confirmed through autocorrelational analysis of fluorescence signals on each detection channel and cross-correlation analysis between the two color channels.

Therefore, the FCCS scheme reported herein can obviate the need for negative control experiments with mathematical corrections and their complications that can reduce assay turn-around time as well as data quality typically required to correct impaired data arising from spectral cross-emission.¹⁹ Because no cross-excitation and/or FRET was observed, this will provide better control of each excitation laser power while preventing photobleaching, which can be a challenge in single laser FCCS²² or two-photon excitation FCCS.²³⁻²⁵ Furthermore, it can increase the data quality by ensuring that all the coincidence events are truly double-labeled molecules.

The feasibility of this FCCS system was demonstrated by comparing the relative amplitudes of the cross-correlation functions through the nicking of a dsDNA substrate at abasic sites by APE1, with and without CRT0044876 a known inhibitor of APE1, using FCCS. The ability of APE1 to incise abasic sites in the BER pathway has been evaluated using FCCS without the need for gel electrophoresis, which is a common assay method requiring longer assay times to confirm enzyme activity compared to FCCS.⁴¹⁻⁴²

While the current FCCS measurements used a 30 min enzymatic incubation step, this incubation time can be significantly reduced using smaller reaction volumes (*i.e.*, lower diffusional distances), reduced dispersion, and/or rapid mixing, such as those typically employed in many microfluidic platforms with multi-phase flows.⁴³⁻⁴⁵ Furthermore, in many high throughput applications for drug discovery, multiple potential target inhibitors must be simultaneously analyzed. Therefore, the FCCS system with single-molecule sensitivity reported herein can be configured using microfluidics to perform multi-channel measurements in which many drug candidates can be simultaneously analyzed in near real-time similar to the cartridge-based screening format.⁴⁶ The sample processing throughput of the present system, which was performed in a single-channel format, was estimated to be $\sim 3,360$ molecules s^{-1} . However, this sampling throughput could be significantly increased when configured in a multi-channel format; using a 200 μm field of view and a series of fluidic channels with widths and pitches near the diffraction limit would provide a single-molecule sampling throughput of $9.6 \times 10^5 s^{-1}$ (see Supporting Information for calculation).⁴⁷⁻⁴⁸

Supplementary Material

Refer to Web version on PubMed Central for supplementary material.

Acknowledgments

The authors acknowledge financial support of this work through the National Institutes of Health (EB-006639), the National Science Foundation (EPS-0346411) and the Louisiana Board of Regents.

References

1. Wang Z, Shah J, Chen Z, Sun C, Berns M. J Biomed Opt 2004;9:395. [PubMed: 15065907]
2. Kim S, Heinze K, Waxham M, Schwille P. Proc Natl Acad Sci USA 2004;101:105–110. [PubMed: 14695888]
3. Bacia K, Kim SA, Schwille P. Nat Methods 2006;3:83–89. [PubMed: 16432516]
4. Bacia K, Majoul I, Schwille P. Biophys J 2002;83:1184–1193. [PubMed: 12124298]

5. Jung J, Van Orden A. *J Am Chem Soc* 2006;128:1240–1249. [PubMed: 16433541]
6. Schubert F, Zettl H, Hafner W, Krauss G, Krausch G. *Biochem* 2003;42:10288–10294. [PubMed: 12939158]
7. Magde D, Elson E, Webb W. *Phys Rev Lett* 1972;29:705–708.
8. Doose S, Tsay J, Pinaud F, Weiss S. *Anal Chem* 2005;77:2235–2242. [PubMed: 15801758]
9. Kral T, Langner M, B M, Baczynska D, Ugorski M, Hof M. *Biophys Chem* 2002;95:135–144. [PubMed: 11897152]
10. Hegener O, Jordan R, Haberlein H. *J Med Chem* 2004;47:3600–3605. [PubMed: 15214787]
11. Schwille P, Haustein E. Fluorescence correlation spectroscopy An introduction to its concepts and applications. *Biophysics Textbook Online*. 2001
12. Zander, C.; Enderlein, J.; Keller, R. *Single molecule detection in solution*. Wiley-VCH; Weinheim: 2002.
13. Kettling U, Koltermann A, Schwille P, Eigen M. *Proc Natl Acad Sci USA* 1998;95:1416–1420. [PubMed: 9465029]
14. Eigen M, Rigler R. *Proc Natl Acad Sci USA* 1994;91:5740–5747. [PubMed: 7517036]
15. Haustein E, Schwille P. *Annu Rev Biophys Biomol Struct* 2007;36:151–169. [PubMed: 17477838]
16. Schwille P, Meyer-Almes F, Rigler R. *Biophys J* 1997;72:1878–1886. [PubMed: 9083691]
17. Foldes-Papp Z, Rigler R. *Biol Chem* 2001;382:473–478. [PubMed: 11347895]
18. Kogure T, Karasawa S, Araki T, Saito K, Kinjo M, Miyawaki A. *Nat Biotechnol* 2006;24:577. [PubMed: 16648840]
19. Bacia K, Schwille P. *Nat Protocols* 2007;2:2842–2856.
20. Foldes-Papp Z. *Curr Pharm Biotechnol* 2005;6:437. [PubMed: 16375728]
21. Takahashi Y, Nishimura J, Suzuki A, Ishibashi K, Kinjo M, Miyawaki A. *Cell Struct Funct* 2008;33:143–150. [PubMed: 18931453]
22. Hwang LC, Wohland T. *ChemPhysChem* 2004;5:549–551. [PubMed: 15139229]
23. Heinze KG, Koltermann A, Schwille P. *Proc Natl Acad Sci USA* 2000;97:10377–10382. [PubMed: 10973482]
24. Swift J, Heuff R, Cramb D. *Biophys J* 2006;90:1396–1410. [PubMed: 16299079]
25. Kim S, Heinze K, Bacia K, Waxham M, Schwille P. *Biophys J* 2005;88:4319–4336. [PubMed: 15792970]
26. Thews E, Gerken M, Eckert R, Zapfel J, Tietz C, Wrachtrup J. *Biophys J* 2005;89:2069–2076. [PubMed: 15951373]
27. Kogure T, Karasawa S, Araki T, Saito K, Kinjo M, Miyawaki A. *Nat Biotechnol* 2006;24:577–581. [PubMed: 16648840]
28. Demple B, Harrison L. *Annu Rev Biochem* 1994;63:915–948. [PubMed: 7979257]
29. Alseth I, Eide L, Pirovano M, Rognes T, Seeberg E, Bjoras M. *Mol Cell Biol* 1999;19:3779–3787. [PubMed: 10207101]
30. McNeill D, Narayana A, Wong H, Wilson D III. *Environ Health Perspect* 2004;112:799–804. [PubMed: 15159209]
31. Davis L, Williams P, Ball D, Swift K, Matayoshi E. *Curr Pharm Biotechnol* 2003;4:451–462. [PubMed: 14683437]
32. Soper SA, Mattingly QL, Vegunta P. *Anal Chem* 1993;65:740–747.
33. Dorre K, Stephan J, Lapczynska M, Stuke M, Dunkel H, Eigen M. *J Biotechnol* 2001;86:225–236. [PubMed: 11257533]
34. Burkhardt M, Heinze KG, Schwille P. *Opt Lett* 2005;30:2266–2268. [PubMed: 16190439]
35. Hill E, Mello A. *The Analyst* 2000;125:1033–1036.
36. Foldes-Papp Z. *Exp Mol Pathol* 2007;82:147–155. [PubMed: 17258199]
37. Niethammer P, Kronja I, Kandels-Lewis S, Rybina S, Bastiaens P. *PLoS Biol* 2007;5:190–202.
38. Markham N, Zuker M. *Nucleic Acids Res* 2005;33:W577. [PubMed: 15980540]
39. Bahr U, Karas M, Hillenkamp F. *Anal Bioanalytical Chem* 1994;348:783–791.
40. Tang K, Fu D, Kotter S, Cotter R, Cantor C. *Nucleic Acids Res* 1995;23:3126. [PubMed: 7667088]

41. Madhusudan S, Smart F, Shrimpton P, Parsons J, Gardiner L, Houlbrook S, Talbot D, Hammonds T, Freemont P, Sternberg M. *Nucleic Acids Res* 2005;33:4711. [PubMed: 16113242]
42. Masuda Y, Bennett R, Demple B. *J Biol Chem* 1998;273:30352–30359. [PubMed: 9804798]
43. Song H, Tice J, Ismagilov R. *Angew Chem* 2003;42:768. [PubMed: 12596195]
44. Li L, Boedicker J, Ismagilov R. *Anal Chem* 2007;79:2756. [PubMed: 17338503]
45. Yoshida A, Urasaki Y, Waltham M, Bergman A, Pourquier P, Rothwell D, Inuzuka M, Weinstein J, Ueda T, Appella E. *J Biol Chem* 2003;278:37768–37776. [PubMed: 12842873]
46. Chen D, Ismagilov R. *Curr Opin Chem Biol* 2006;10:226–231. [PubMed: 16677848]
47. Emory J, Soper S. *Anal Chem* 2008;80:3897–3903. [PubMed: 18412372]
48. Okagbare P, Soper S. *The Analyst* 2009;134:97. [PubMed: 19082181]

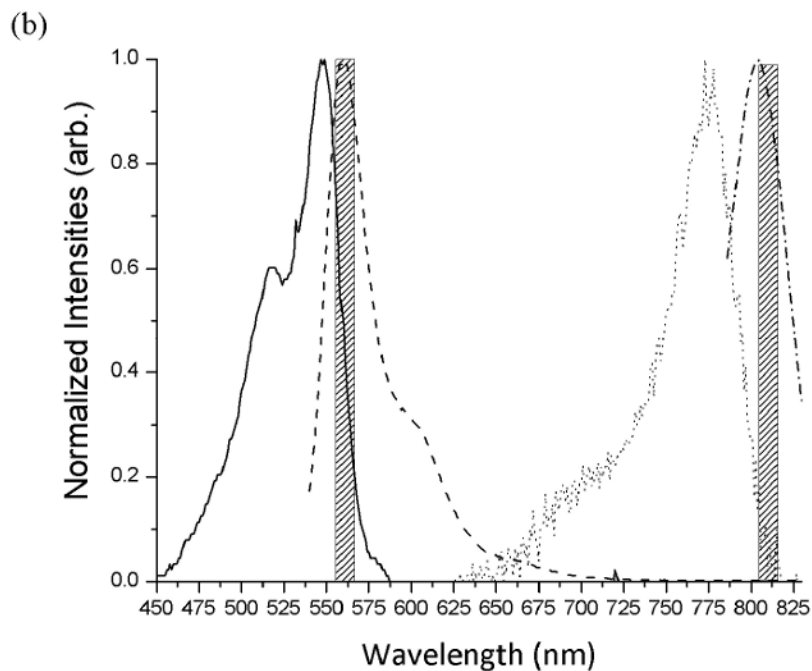
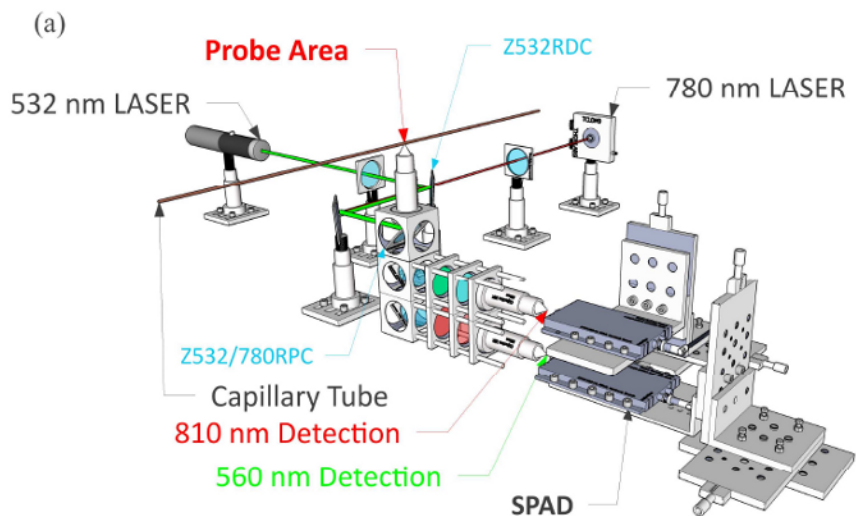
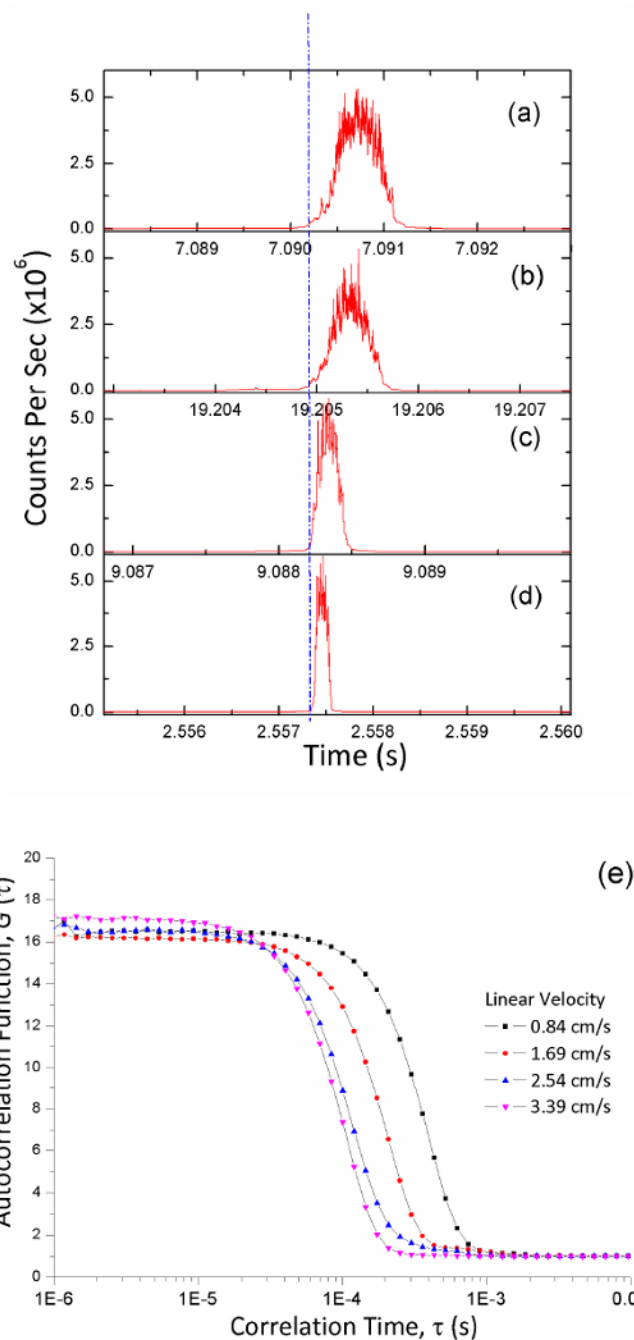


Figure 1.

(a) Schematic of the instrumental setup for implementing dual-color FCCS. Two collinear excitation beams at 532 nm and 780 nm were focused through a 40 \times , 0.75 NA objective into a 50 μ m internal diameter fused silica capillary. The dual color fluorescence was subsequently processed on two different color-channels (centered at 560 nm and 810 nm) containing SPADs. (b) Absorption (solid line) and emission (dashed line) spectra of a Cy3-labeled oligonucleotide and absorption (dotted line) and emission (dash-dotted line) spectra of an IRD800-labeled oligonucleotide. The pass band of the filters used for each color channel is shown as well.

**Figure 2.**

Single particle events (fluorescent spheres and quantum dots) monitored using the dual-color instrument sampled at various volumetric flow rates ranging from 1.0 $\mu\text{l/min}$ to 4.0 $\mu\text{l/min}$. Comparison of a fluorescence event from a particle moving through the excitation beam (532 nm) at 1 $\mu\text{l/min}$ (a), 2 $\mu\text{l/min}$ (b), 3 $\mu\text{l/min}$ (c), and 4 $\mu\text{l/min}$ (d). (e) Autocorrelation plots for single particle events at different volume flow rates ranging from 1.0 $\mu\text{l/min}$ (linear velocity = 0.84 cm/s) to 4 $\mu\text{l/min}$ (linear velocity = 3.39 cm/s).

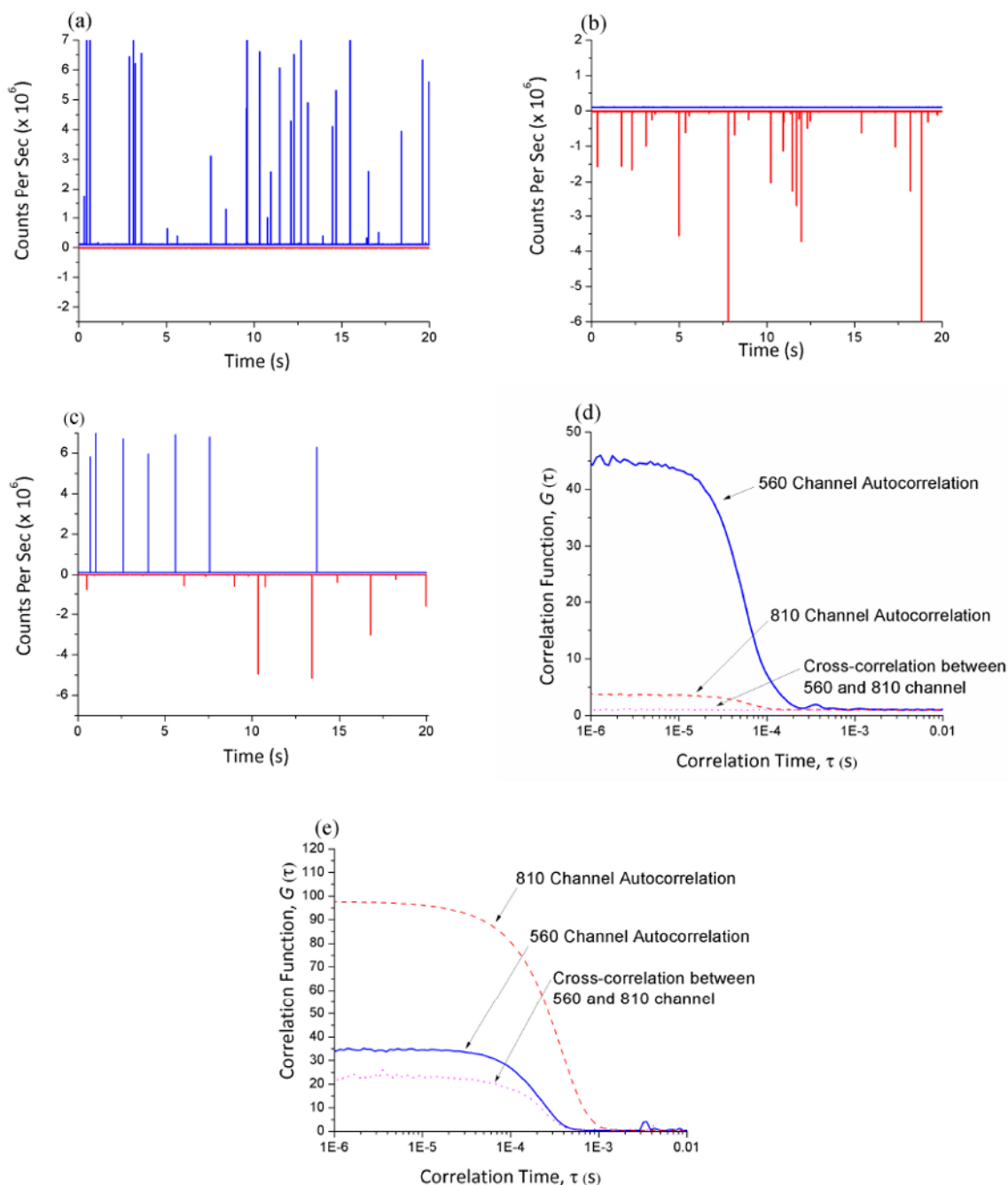
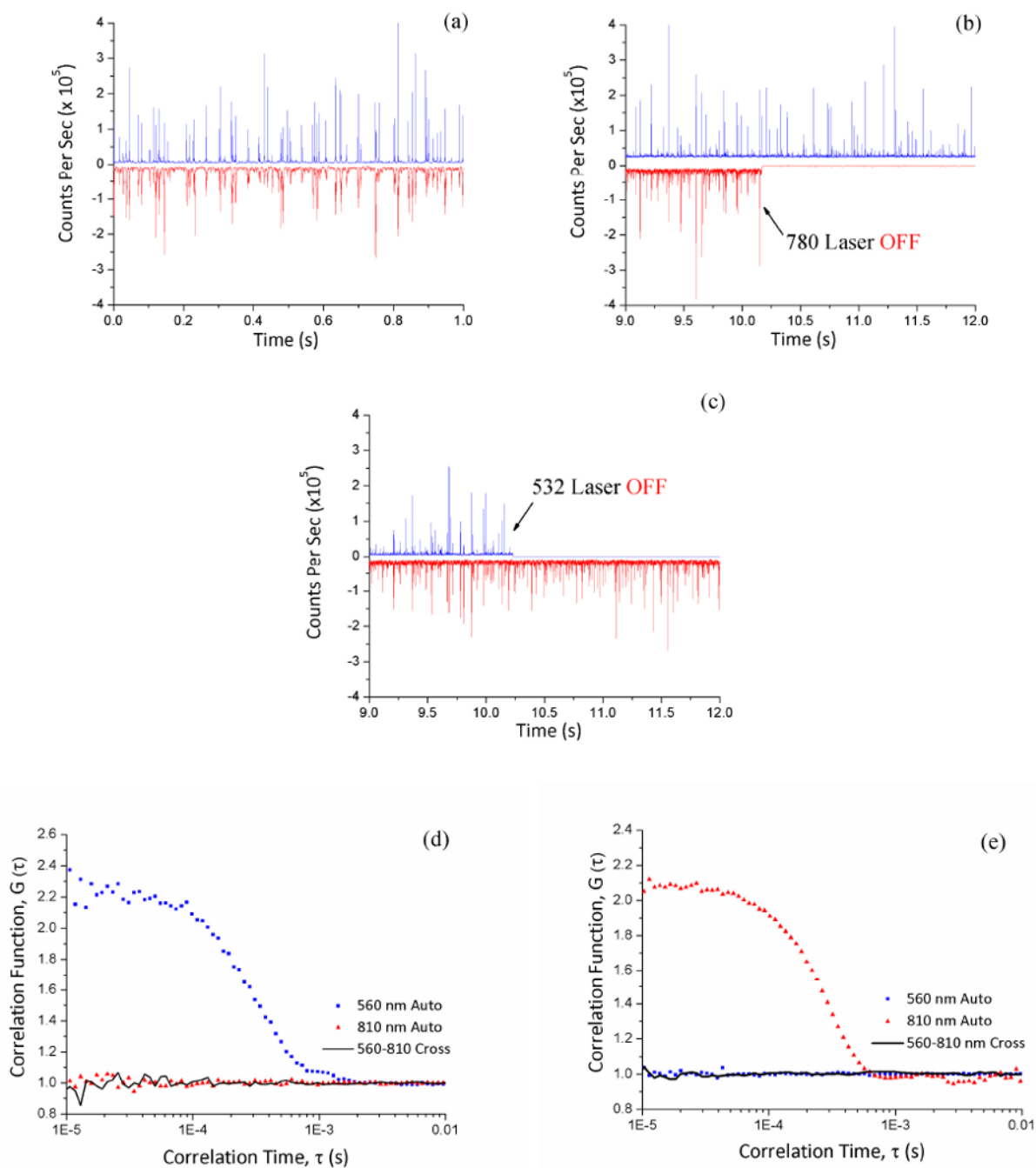


Figure 3.

Data streams showing single particle events when transported hydrodynamically through the sampling capillary for; (a) fluorescent spheres only (4.5×10^5 particles/ml); (b) quantum dots only (2.5×10^{-9} mg/ml); and (c) a mixture of the spheres and quantum dots (8.6×10^4 particles/ml for spheres and 1.0×10^{-9} mg/ml for quantum dots). (d) Autocorrelation functions and a cross-correlation function for a mixed particle (spheres and quantum dots) sample (top trace is signal from the 560 nm detection channel and the bottom trace is for the 810 nm detection channel).

**Figure 4.**

Single molecule data streams for the dsDNA substrate labeled with Cy3 (positive trace) and IRD800 (negative trace) monitored using the dual-color instrument. (a) The dsDNA substrate at 0.3 pM labeled with Cy3 and IRD800 at opposite ends was hydrodynamically transported through the 50 μ m capillary with both excitation beams illuminating the sample continuously. (b) During the measurement, the 780 nm laser was switched off at ~10 s into the data stream. (c) The excitation beam at 532 nm was switched off at ~10 s into the data stream. (d) Plots of the autocorrelation functions and a cross-correlation function for the Cy3-labeled ssDNA only.

(e) Plots of the autocorrelation functions and a cross-correlation function for an IRD800-labeled ssDNA only.

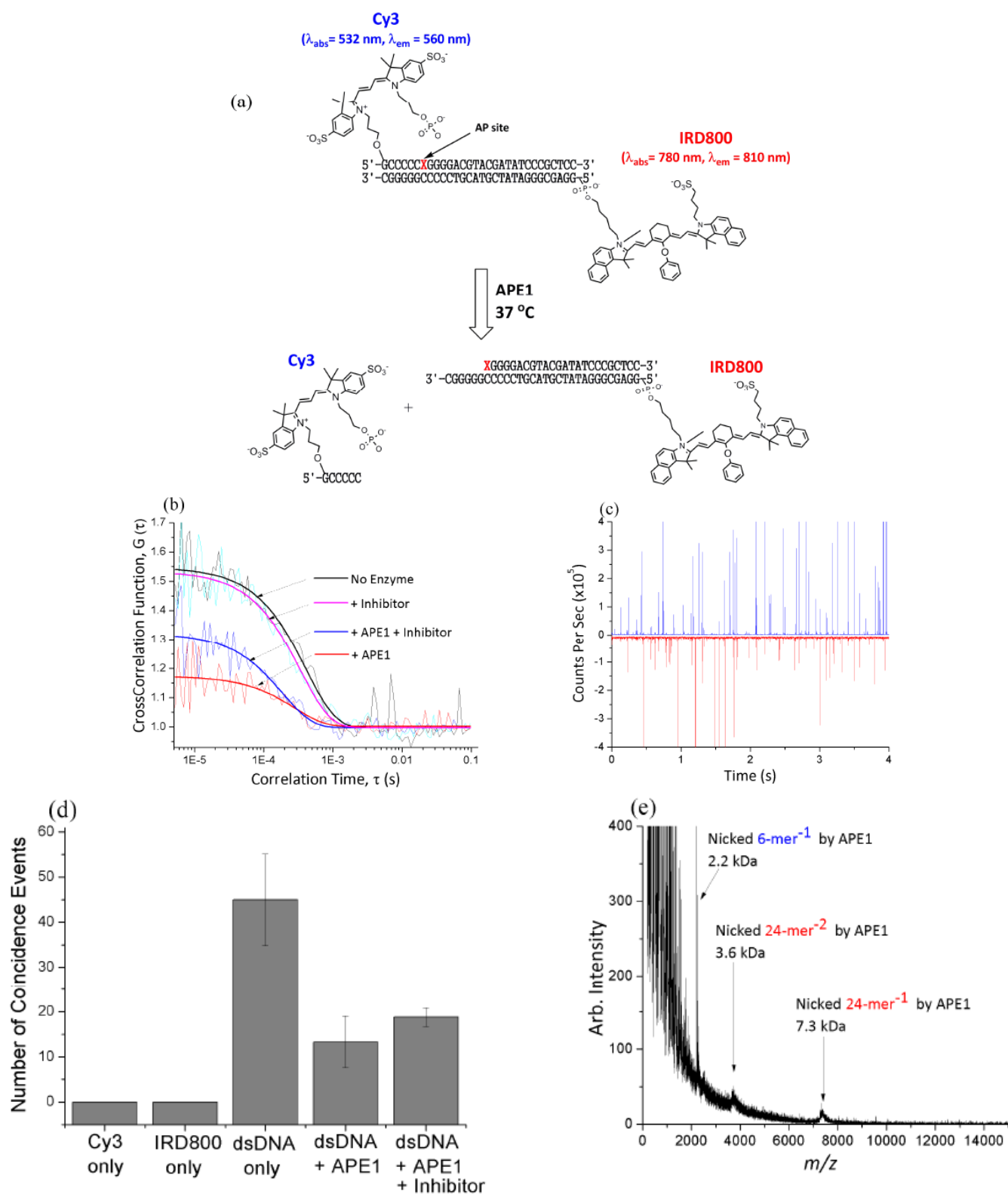


Figure 5.

(a) Representation of the FCCS assay for evaluating APE1 activity. Two synthetic, 30 nt complementary oligonucleotides containing an abasic site (tetrahydrofuran) at position 7 in the upper strand were labeled at their 5' ends with Cy3 and IRD800. (b) Fluorescence cross-correlation functions of various combinations of samples showing the activity of APE1 in the presence and absence of a known inhibitor. The duplex at 0.3 pM in the BER reaction buffer were prepared by adding APE1 enzyme (1 nM) and/or inhibitor (2 mM) and then incubated for 30 min at 37°C prior to the FCCS measurements. The data were fit by a Levenberg-Marquardt nonlinear least square method. (c) Single molecule data streams for the duplex DNA substrate labeled with Cy3 (positive trace) and IRD800 (negative trace) at 1.0 μ L/min when incubated with APE1. (d) Comparison of number of coincident events ($n = 4$) during the 20 s acquisition time. (e) Negative-ion MALDI mass spectrum of 6-mer (5'-Cy3-GCCCCC, 2219.7 Da) and 24-mer (XGGGGACGTACGATATCCCGCTCC-3', 7266.2 Da) APE1 enzymatic products. The matrix was 3-HPA in 50% acetonitrile.